Structure of the Magnetic Trilayer System Fe/Pd/Fe Epitaxially Grown on GaAs(001)-4 × 6

P.S. Budnik[1], R.A. Gordon[1], E.D. Crozier[1]
[1]Physics Department, Simon Fraser University, Burnaby, B.C., V5A 1S6, Canada

Introduction

The magnetic behaviour of ferromagnetic/non-ferromagnetic/ferromagnetic trilayers is strongly dependent on the nature of the interface between layers, the strain in the layers and the extent of any interdiffusion or reaction between layers and substrate. The MBE facility at the PNC-CAT ID line permits epitaxial layer-by-layer growth and structural characterization at any stage of the growth. In this report, results are presented from a polarization-dependent *in situ* XAFS study of Fe/Pd/Fe trilayers epitaxially grown on GaAs(001)-(4x6). Fe and Pd K-edge spectra were obtained in total reflection mode. Measurements above and below the critical angle permitted structural determination of underlying Fe(Pd) when covered with a few monolayers of Pd(Fe).

Methods and Materials

Samples on GaAs(001)-(4×6) were prepared *in situ* by MBE on epiready n-type GaAs (American Xtal Technology) wafers as described elsewhere [1, 2]. Layer deposition was monitored by reflection high-energy electron diffraction (RHEED) with the number of oscillations of specular (anti-Bragg) spot intensity giving the layer thickness in ML. These measurements were used as calibration for the rate of deposition.

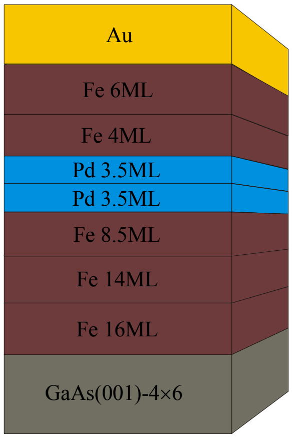

Fig.1. Growth stages of the magnetic trilayer sample.

In growing the Fe/Pd/Fe trilayer sample, Fig.1, a total of 30 ML of Fe were first deposited. Ar^+ sputtering was then used to remove the less than 1 ML of As from the GaAs that is known to float to the surface during Fe deposition [1,3]. The sample was annealed for 30 minutes at ~150° C and another 8.5 ML of Fe were deposited at the anneal temperature. This is referred to as the 38.5ML Fe sample. Subsequently the following overlayers were grown: 3.5 ML Pd; 3.5 ML Pd for a total of 7 ML Pd; 4 ML Fe; and 6 ML Fe for a total of 10 ML Fe. The Fe and Pd deposition rates were ~0.4 ML/min and ~0.3 ML/minute, respectively.

XAFS measurements were made using the PNC-CAT undulator beamline, ID-20 [4]. The Si(111) double-crystal monochromator was detuned above the Fe and Pd K-edges to 75% of the maximum intensity to reduce harmonic contributions. X-rays were incident in the total-reflection geometry with the electric vector either (near) perpendicular, $\mathbf{E}_\perp$, or in the plane of the substrate, $\mathbf{E}_{||}$ (within 2° of (110) and (-110) orientations). To minimize distortion of the spectra due to anomalous dispersion effects in the sample and adjacent media, the angle of incidence was set to approximately 2/3 of the critical angle φ_C at 250 eV above the respective K-edges [5]. Fe K-edge measurements, $\mathbf{E}_{||}$, were also made at ~$2\varphi_C$ after deposition of 3 ML Pd in order to examine the effect of growing overlayers of Pd on the structure of the underlying Fe. All XAFS data on the trilayers were acquired using total electron yield.

The EXAFS interference functions were extracted using AUTOBK [6] while fixing E_o at the first inflection point. Polarization-dependent XAFS amplitudes and phase shifts were calculated using FEFF 7 [7] and non-linear least squares fitting of the Fourier transform of $k\chi(k)$ was done using WINXAS [8].

Results

Detailed analysis, done in R-space, indicates that in our Fe/Pd/Fe trilayer system in all three layers the Fe and Pd are distorted from their natural bcc and fcc structures, respectively. The underlying Fe, consistent with previous results [1,2], has a bct structure with c/a=1.03 and a=2.83Å. Alloy is formed at both Fe/Pd and Pd/Fe interfaces. The amount of alloying is smaller at the first interface compared to the second. Main aspects of the analysis are given below.

The magnitudes of the Fourier transforms of kχ(k) for the Pd data are shown in Fig. 2. Polycrystalline Pd has a fcc structure with n.n. distance $R_1 = 2.75$ Å and second n.n. $R_2 = 3.89$ Å.

The splitting of the main peak into A and B is produced by the k-dependence of the Pd backscattering amplitude, f(k,π), when convolved with the n.n. distribution function. Using FEFF 7 the offset between the fit and crystallographic distances for Pd foil are ~ 0.01Å for $R_1$and 0.03 Å for R_2. Inspection of Fig. 2 reveals the peak ratio B/A decreases as the thickness of the film decreases. This is caused by backscattering from the underlying Fe, some of which has alloyed with Pd.

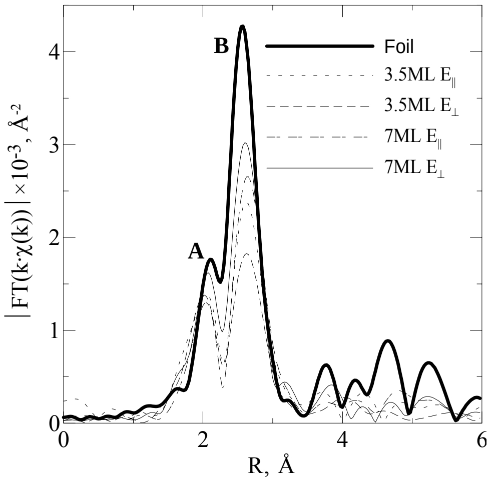

Fig. 2. The magnitude of the Fourier transform of kχ(k) for the Pd films and Pd foil. The transforms were calculated with a 20% Gaussian window over the k-space range 2.3 – 12.3 $Å^{-1}$.

Fig. 3 shows the result of fitting 3.5 ML Pd with the electric vector parallel to the substrate. The solid line is the magnitude of the FT of the data. The long-dashed and dotted lines are the imaginary parts of the Pd-Fe and Pd-Pd contributions to the fit of the data, respectively. The broken line indicates the magnitude of the fit including the n.n. Pd-Fe distance and three Pd-Pd distances out to 4.7 Å.

The imaginary parts of the Fourier transform for Pd-Fe and Pd-Pd are almost in-phase under peak A but become out-of-phase under peak B. This interference makes the fit sensitive to the Pd-Fe interface.

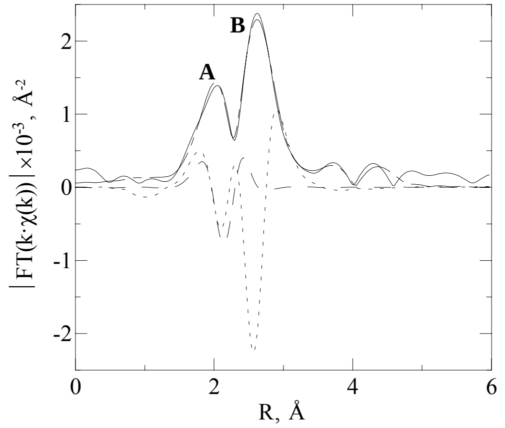

Fig. 3. The contribution of Fe and Pd to the transform of 3.5 ML Pd in the $\mathbf{E}_{\|}$ configuration.

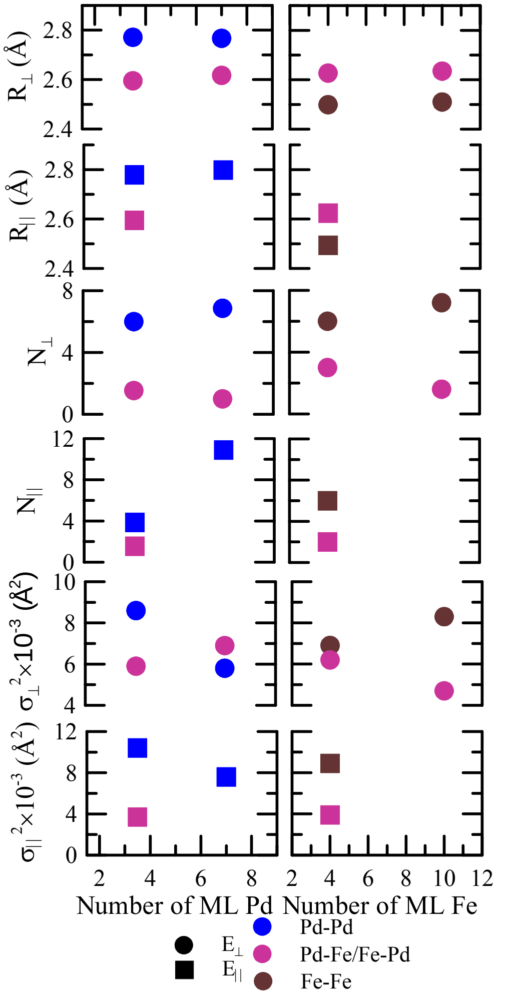

Fig. 4. R, N and σ^2 for both polarizations are shown as a function of number of monolayers of Pd (left) and Fe (right).

Obtained fitting parameters (R, N, σ^2) for the first shell of Pd and Fe for both E perpendicular and parallel are shown the Fig. 4. Together with parameters for the second and third shells (not shown) they indicate bct structures for both the Fe underlayer and overlayer, and a fct structure of the Pd interlayer. Pd-Fe (Fe-Pd) distances and coordination numbers give insight into the nature of the Fe/Pd (Pd/Fe) interfaces and the extent of interface alloying.

Discussion

Analysis of $\mathbf{E}_{\perp}$ and $\mathbf{E}_{||}$ for the 3.5ML Pd sample revealed that Pd has a fct structure expanded in-plane and contracted out-of-plane (with respect to fcc Pd) with a=3.93 Å and c=3.87 Å. In the growth of Pd on bct Fe, the Pd fcc lattice can be considered as a bct structure with in-plane lattice parameter being smaller than the underlying Fe in-plane lattice. The Pd fcc lattice rotates 45° with respect to the Fe bct lattice and expands in-plane in attempt to match Fe. This causes contraction in the out-of-plane direction at the same time.

Both polarizations indicate the presence of Fe under the first peak of the Fourier transform. The coordination number for the n.n. Pd-Fe distance and this distance itself, 2.60 Å (same for both polarizations) suggest the formation of an alloy within the first 0.5 – 1 ML Pd, as shown in Fig. 5.

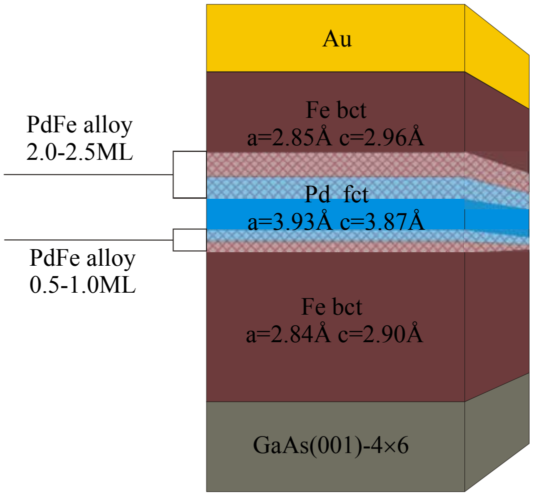

Fig. 5 Structure of Fe/Pd/Fe magnetic trilayer.

Analysis of 7ML Pd showed that the fct structure of Pd is preserved. Analysis of $\mathbf{E}_{||}$ showed no presence of Fe, while $\mathbf{E}_{\perp}$ revealed a small amount of Fe, correlated through coordination numbers and Pd-Fe distance with the 3.5ML Pd data, allowing one to speculate that no further alloying between Fe and Pd occurred when the additional 3.5ML of Pd were deposited.

Analysis of the upper 4ML Fe, both $\mathbf{E}_{||}$ and $\mathbf{E}_{\perp}$, revealed Pd to be present in greater amounts than the traces of Fe at the 38.5MLFe/Pd interface. Coordination numbers yield around 2-2.5ML of Fe-Pd alloy consistent with XAFS results for Fe deposited on Pd(001) grown on MgO substrate [9]. Fe-Fe distances show that Fe has a bct structure with a=2.85 Å and c=2.96 Å which is more distorted from bcc than Fe grown on GaAs(001)-(4x6). Analysis of $\mathbf{E}_{\perp}$ for 10ML of Fe, is in agreement with the 4ML data, showing the same tetragonal distortion and the presence of some Pd. The Fe-Pd n.n. distance stays the same as for the 4ML sample and equal to 2.63 Å.

Acknowledgments

This work was supported by the Natural Sciences and Engineering Research Council of Canada through major facilities access and operating grants**.** Research at the PNC-CAT beamline, Advanced Photon Source, Argonne National Laboratory is also supported by the US Department of Energy under contracts W-31-109-Eng-38 (APS) and DE-FG03-97ER45628 (PNC-CAT).

References

1. Gordon, R.A., Crozier, E.D., Jiang, D.-T., Monchesky, T.L. and Heinrich, B., Phys. Rev. B **62**, 2151 (2000).
2. Gordon, R.A., Budnik, P.S., Jiang D.T., Crozier, E.D., XAFS 12 conference proceedings.
3. Monchesky, T.L., Heinrich, B., Urban, R., Myrtle, K., Klaua, M. and Kirschner, J., Phys. Rev. B **60**, 10242 (1999).
4. Heald, S., Stern, E.A., Brewe, D., Gordon, R., Crozier, E. D., Jiang, D.T and Cross, J., J. Synch. Rad. **8**, 342 (2001)
5. Jiang, D.T. and Crozier, E.D., Can. J. Phys. **76**, 621 (1998).
6. Newville, M., Livins, P., Yacoby, Y.,Stern , E.A., and Rehr, J.J., Phys. Rev. B. **47** 14126 (1993).
7. Zabinsky, S.I., Rehr, J.J., Ankudinov, A., Albers, R.C., and Eller, M.J., Phys. Rev. B **52**, 2995 (1995).
8. Ressler, T., J. Phys. IV **7**, C2-269 (1997).
9. Boeglin, C. *et al*, Phys. Rev. **B 60** 4220 (1999).